

# Hall Effect in Nested Antiferromagnets Near the Quantum Critical Point

M. R. Norman<sup>1</sup>, Qimiao Si<sup>2</sup>, Ya. B. Bazaliy<sup>1</sup>, and R. Ramazashvili<sup>1</sup>

<sup>1</sup>*Materials Science Division, Argonne National Laboratory, Argonne, Illinois 60439*

<sup>2</sup>*Department of Physics and Astronomy, Rice University, Houston, Texas 77005-1892*

(Dated: November 11, 2018)

We investigate the behavior of the Hall coefficient in the case of antiferromagnetism driven by Fermi surface nesting, and find that the Hall coefficient should abruptly increase with the onset of magnetism, as recently observed in vanadium doped chromium. This effect is due to the sudden removal of flat portions of the Fermi surface upon magnetic ordering. Within this picture, the Hall coefficient should scale as the square of the residual resistivity divided by the impurity concentration, which is consistent with available data.

PACS numbers: 72.15.Eb, 75.10.Lp, 71.10.Hf, 71.18.+y

There has been recent interest, both experimentally[1, 2] and theoretically[3, 4], in the physics of magnetic quantum critical points (QCPs). Such QCPs occur when the ordering temperature of a magnet has been driven to zero continuously by some tuning parameter, such as chemical doping. Much of the interest is due to strong signatures of non-Fermi liquid behavior near QCPs, and the difficulties of standard theories of itinerant magnetism in explaining such behavior. In the case of heavy fermion metals, there is some indication that the QCP is accompanied by localization of the *f* electrons[1, 2, 3, 4]. This should result in a volume change of the Fermi surface. A novel signature of non-trivial QCPs is a jump in the Hall coefficient [3, 4]. In the case of heavy fermions, results are still preliminary at this time[5]. Related issues are also being discussed for high temperature superconductors[6, 7].

Recently, Yeh *et al.*[8] studied the Hall coefficient in the simpler case of V-doped Cr. Upon doping with V, the Néel temperature is rapidly suppressed to zero, leading to a QCP at about 4% doping. The Hall coefficient decreases, quite abruptly, by about a factor of two with doping into the paramagnetic phase. Both the magnitude and the abruptness of this change are surprising, given that Cr is well established to be a simple spin-density-wave magnet. One of the characteristic features of Cr is that its Fermi surfaces are nested. Indeed, magnetism in Cr is traditionally understood as being driven by nesting.

In this paper, we show that the magnitude of the change in the zero-temperature Hall coefficient across the magnetic QCP can be quantitatively accounted for by the removal of the flat portions of the Fermi surface upon magnetic ordering. From this picture, it follows that the zero-temperature Hall coefficient should scale as the square of the residual resistivity divided by the impurity concentration, and we demonstrate that the available data in V-doped Cr are consistent with such a relationship. Our results establish that the Fermi-surface nesting picture is quantitatively correct for zero-temperature properties, thereby providing a solid foundation for further understanding of the non-Fermi liquid behavior in this benchmark quantum critical metal.

The Hall conductivity is in general a component of a tensor object. In the case of cubic materials, such as Cr, only one component is relevant. In this paper, we will confine our discussion to the level of Boltzmann approximation, which should be adequate for the zero-temperature limit even when interactions are significant. Within this approximation, the Hall coefficient is

$$R_H = \sigma_{xyz} / \sigma_{xx}^2 \quad (1)$$

where[9],

$$\sigma_{xyz} = \frac{e^3 \tau^2}{\hbar \Omega c} \sum_{\vec{k}} v_x (\vec{v} \times \vec{\nabla}_k)_z v_y \left( -\frac{\partial f}{\partial \epsilon_k} \right) \quad (2)$$

$$\sigma_{xx} = \frac{e^2 \tau}{\Omega} \sum_{\vec{k}} v_x^2 \left( -\frac{\partial f}{\partial \epsilon_k} \right) \quad (3)$$

Here,  $1/\tau$  is the scattering rate,  $\Omega$  the volume, and  $f$  the Fermi distribution function.

The physical picture we propose is as follows. It is known that parts of the Cr Fermi surface are flat and nested, and the remaining parts are regular. The magnetic ordering gaps out the flat surfaces. We note that Eq. (2) is a weighted sum of various components of the inverse mass tensor; the latter measures the curvature of the Fermi surface. Therefore, the flat Fermi surface sheets will make a small contribution to  $\sigma_{xyz}$  even in the paramagnetic state. Thus, upon magnetic ordering,  $\sigma_{xyz}$  is not expected to change much. On the other hand,  $\sigma_{xx}$  involves only components of the velocity and would contain considerable contributions from the flat Fermi surface sheets in the paramagnetic phase. Removal of the flat Fermi surfaces upon magnetic ordering should lead to a large change in  $\sigma_{xx}$ . This will be amplified in the Hall coefficient, since the square of  $\sigma_{xx}$  appears in Eq. (1). Such reasoning makes clear a very general relationship between the the Hall coefficient and the longitudinal resistivity across the QCP.

At  $T = 0$ , the inverse of  $\sigma_{xx}$  is the residual resistivity,  $\rho_0$ . Therefore, we expect scaling between  $R_H$  and  $\rho_0$ . If

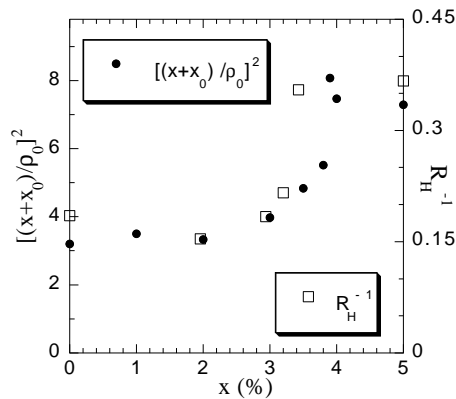


FIG. 1: Doping dependence of the Hall number ( $R_H^{-1}$ , carriers per unit cell) [8] and of the inverse square of the residual resistivity ( $\rho_0$ ,  $\mu\Omega$  cm) [10].  $\rho_0$  is divided by the effective impurity concentration,  $x + x_0$ , where  $x$  is the doping, and  $x_0 = 0.59\%$  the impurity concentration at stoichiometry, determined from a linear fit of  $\rho_0$  at low doping. The discrepancy between the plots is largely due to the different critical concentrations of the two sample sets (3.5% for the Hall samples, 4% for the resistivity samples). The experimental  $R_H$  point at 5% doping actually corresponds to 10% doping, and is shown simply to illustrate the approximate constancy of  $R_H$  in the paramagnetic phase.

the tuning parameter (such as pressure) does not change the elastic scattering, it follows that

$$\frac{R_H^{pm}}{R_H^{afm}} = \left( \frac{\rho_0^{pm}}{\rho_0^{afm}} \right)^2 \quad (4)$$

where the superscripts “pm” and “afm” refer to the paramagnetic and antiferromagnetic phases, respectively. When the transition is induced by doping, the elastic scattering is also being changed, presumably in a linear fashion. For impurities that are intermediate between Born and unitarity limits, we find that

$$\frac{R_H^{pm}}{R_H^{afm}} = \left( \frac{d\rho_0^{pm}/dx}{d\rho_0^{afm}/dx} \right)^2 \quad (5)$$

From data available in the literature[10], the concentration dependence of  $\rho_0$  goes as  $x + x_0$ , where  $x_0$  represents impurities already present in the stoichiometric material. We can check the validity of Eq. (5) by comparing  $(x + x_0)/\rho_0$  with the Hall number,  $R_H^{-1}$ . As seen in Fig. 1, the correlation is quite good. The discrepancy is mainly due to the fact that the resistivity was measured on a sample with critical point at about 4% doping, whereas the Hall data were taken on samples with the critical doping of 3.5%. It would be important to test Eq. (5) in greater detail by taking Hall and resistivity data on the same samples. We also note that Eq. (4) is consistent with the pressure data [11].

We now turn to quantitative considerations of the Hall coefficient itself. To this effect, we have performed band

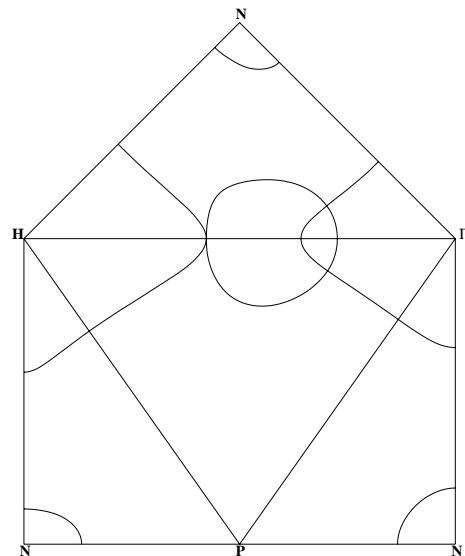


FIG. 2: Fermi surface of Cr plotted in the faces of the irreducible wedge of the BCC zone. In units of  $\pi/a$ , the symmetry points correspond to  $\Gamma$  (0,0,0),  $H$  (2,0,0),  $N$  (1,1,0), and  $P$  (1,1,1). The Fermi surface consists of a  $\Gamma$  centered electron octahedron, an  $H$  centered hole octahedron,  $N$  centered hole ellipsoids, and  $\Gamma - H$  centered electron balls.

calculations within the local density approximation for Cr, using the linear muffin tin orbital method. After self-consistent convergence, eigenvalues were generated on a 506 k point grid in the irreducible wedge (1/48th) of the BCC Brillouin zone. These eigenvalues were then interpolated using a 910 function Fourier series (spline fit). The resulting Fermi surface is shown in Fig. 2. It consists of four parts, a  $\Gamma$  centered electron octahedron, an  $H$  centered hole octahedron,  $\Gamma - H$  centered electron balls, and  $N$  centered hole ellipsoids. As is well known, the two octahedron surfaces match up when translated by the magnetic  $\mathbf{Q}$  vector. The “gapping out” of these two surfaces by the magnetic ordering has been recently observed by photoemission[12].

We show a Fermi surface decomposition of Eqs. (1-3) in Table 1. We see that although the two flat surfaces make up 40% of the density of states, and 52% of  $\sigma_{xx}$ , they only make up 22% of  $\sigma_{xyz}$ . The total Hall number corresponds to 0.54 (in units of carrier concentration), somewhat larger than the paramagnetic value of 0.37 found for 10% V doping[8]. Actually, the theoretical value decreases with V doping (simulated by a rigid band adjustment of the Fermi energy), and has a value of 0.47 for 10% hole doping.

If the two octahedron surfaces were completely flat, they would be immediately removed by magnetic ordering. The Hall number would then jump from 0.54 to 0.16. (The latter value is identical to experimental values in the magnetic phase[8].) This can be seen from Fig. 3. In Fig. 3a, we show a schematic electronic disper-

TABLE I: Decomposition of the transport integrals for undoped Cr in the paramagnetic phase. DOS is the density of states,  $\sigma_{xx}$  and  $\sigma_{xyz}$  are defined in Eqs. 1-3.  $N - ell$  are the  $N$  centered hole ellipsoids,  $H - octa$  the  $H$  centered hole octahedron,  $\Gamma - octa$  the  $\Gamma$  centered electron octahedron, and  $\Gamma - ball$  the  $\Gamma - H$  centered electron balls. Flat is the sum of the two octahedra, non-flat the sum of the rest. Values listed are the fraction of the total. The resulting Hall number is 0.54, which would be 0.16 if the flat surfaces are eliminated.

	$N - ell$	$H - octa$	$\Gamma - octa$	$\Gamma - ball$	flat	non-flat
DOS	0.12	0.19	0.21	0.48	0.40	0.60
$\sigma_{xyz}$	1.06	0.36	-0.14	-0.29	0.22	0.78
$\sigma_{xx}$	0.27	0.36	0.16	0.21	0.52	0.48

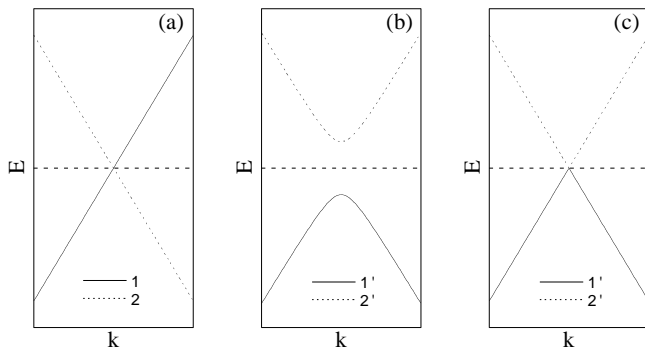


FIG. 3: Schematic of energy bands in Cr. (a) paramagnetic phase - band 1 represents the electron octahedron, band 2 the hole octahedron translated by the magnetic wavevector,  $\mathbf{Q}$ . (b) antiferromagnetic phase - The two bands mix, forming new energy bands 1' and 2' with an energy gap. (c) limit of (b) as the energy gap is taken to zero. Note the different band indexing in (c) as compared to (a). The implication of this for transport integrals is discussed in the text.

sion corresponding to the electron octahedron band of Cr. Also shown in the schematic is the dispersion of the hole octahedron band translated by the magnetic wavevector  $\mathbf{Q}$ . The  $\mathbf{Q}$  vector needed for the crossing point to be degenerate with the Fermi energy will depend on doping (the wavevector is predicted to be commensurate for electron doping, and increasingly incommensurate with hole doping, as observed experimentally[13]). Upon magnetic ordering, an energy gap will open up between these two bands. If the Fermi energy lies inside the gap, as shown in Fig. 3b, then the contribution of the two bands to the transport integral is removed. For the perfectly flat case, this happens even if the energy gap goes to zero, as in Fig. 3c. That is, in this case, a discontinuity in the Hall number is predicted at the QCP.

In the real band structure, the Fermi surface is not perfectly flat, and so the crossing point shown in Fig. 3 disperses as a function of Fermi surface position. To illustrate this, we have performed numerical calculations of the Hall coefficient versus doping. The most natural

way to do this is by restriction to the magnetic Brillouin zone. However, two problems arise. First, energy gaps will always be present in such calculations because of the finite grid in  $k$  space (this is easily understood from Fig. 3). Second, because of the incommensurability, the zone can be ill defined. Instead, we assume a 2 by 2 secular matrix whose diagonal elements are the eigenvalues of the  $H$  centered octahedron (translated by  $\mathbf{Q}$ ), and the electron octahedron, and whose off-diagonal elements are some constant,  $\Delta$  [14]. Note that in this approximation, the  $\Gamma - H$  centered electron balls and  $N$  centered hole ellipsoids are unaffected by magnetic ordering. The paramagnetic electron structure is assumed to be that at 4% V doping, so that the only doping dependence is given by the magnetism. The latter is represented by a  $\mathbf{Q}$  vector of  $0.909(2\pi/a, 0, 0)$ , obtained from the maximum in the susceptibility gotten from the paramagnetic band eigenvalues (this value agrees with experiment[13]). The gap  $\Delta$  (milli-Rydberg) is assumed [13] to vary as  $4.9 - 1.3x$  (where  $x$  is the hole doping in percent). The results are averaged over the three different  $\mathbf{Q}$  domains.

In Fig. 4, we plot the calculated Hall number as a function of  $x$ . Note the striking similarity to Fig. 1, in particular the abrupt drop in the Hall number near the QCP (we cannot calculate too close to the QCP because of numerical problems which can be understood from Fig. 3c). Although the paramagnetic value is somewhat high, the value in the magnetic phase is quite close to experiment [8].

The two octahedra are quite flat. However, on a finer scale, they have different curvatures, leading to a continuous change of the Hall number near the QCP. This change can be expanded in small gap  $\Delta$ . The coefficients of the expansion are model dependent, but the leading power in  $\Delta$  is universal, and can be easily derived for the spherical case using Eqs. 1-3. For unequal sized spheres which intersect (appropriate for hole doped Cr),  $\delta\sigma_{xx}, \delta\sigma_{xyz} \sim \Delta$  for any direction of current,  $\mathbf{J}$ , and field,  $\mathbf{B}$ , from which  $\delta R_H \sim \Delta$ . For touching spheres, though,  $\delta\sigma_{xx} \sim \Delta$  for  $\mathbf{J} \parallel \mathbf{Q}$ ,  $\delta\sigma_{xx} \sim \Delta^2$  for  $\mathbf{J} \perp \mathbf{Q}$ ,  $\delta\sigma_{xyz} \sim \Delta^2$  for  $\mathbf{B} \parallel \mathbf{Q}$ , and  $\delta\sigma_{xyz} \sim \Delta$  for  $\mathbf{B} \perp \mathbf{Q}$ , from which  $\delta R_H \sim \Delta$  for  $\mathbf{B} \perp \mathbf{Q}$ ,  $\mathbf{J} \perp \mathbf{B}$  and  $\delta R_H \sim \Delta^2$  for  $\mathbf{B} \parallel \mathbf{Q}$ ,  $\mathbf{J} \perp \mathbf{Q}$ . (With domain averaging, all changes would go as  $\sim \Delta$ .) This touching case should not be relevant, though, since it corresponds to where the susceptibility has an inflection point as opposed to a maximum [15]. Our results for  $\sigma_{xx}$  agree with previous results in the case of equal sized spheres [16]. (In the 2D case, similar conclusions for  $R_H$  have been reached in Ref. 6.) Since [13]  $\Delta \sim M_{af} \sim x_c - x$  (where  $M_{af}$  is the antiferromagnetic order parameter) near the critical concentration  $x_c$ ,  $\delta R_H \sim x_c - x$ . (Mean field theory would predict  $\Delta \sim \sqrt{x_c - x}$ , in which case  $\delta R_H \sim \sqrt{x_c - x}$ .) We note that the numerical results of Fig. 4 are consistent with a much more rapid variation ( $\delta R_H \sim (x_c - x)^{1/4}$ ), indicating a significant deviation from the spherical model.

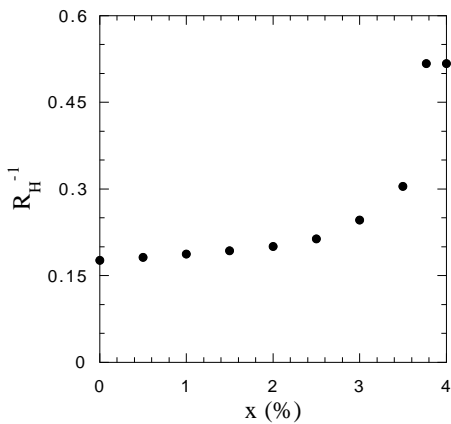


FIG. 4: Calculated Hall number as a function of hole doping.

Although the explanation we give for the behavior of the Hall coefficient seems conventional, the result is consistent with the more exotic physics discussed in Refs. 3, 4. In both cases, the Hall coefficient jumps because of the expectation that the Fermi surface volume changes abruptly at the QCP. In the current case, this is due to nesting. Presumably, in the heavy fermion case, it is due to disconnection of the f electrons from the Fermi surface. Still, the net result for the zero-temperature Hall coefficient is the same. Since entire regions of the Fermi surface are involved in the phase transition, the nesting QCP differs significantly from the standard SDW scenario, where only hot lines of the Fermi surface are relevant. As is now well appreciated, hot lines should not be enough to destabilize the Fermi liquid [17], but if entire regions of the Fermi surface are involved (such as with nesting), the physics changes considerably.

In fact, nesting may be playing a larger role in QCPs than has been appreciated. A recent example is the bilayer ruthenate,  $Sr_3Ru_2O_7$ . This metal exhibits a metamagnetic QCP accompanied by non-Fermi liquid behavior[18]. Recent neutron scattering data find two sets of incommensurate spots, which can be related to Fermi surface nesting[19]. So, it is quite possible that nesting is playing a key role in this system, and perhaps in heavy fermion metals as well.

In conclusion, we have demonstrated that the abrupt change in the zero-temperature Hall coefficient in Cr with V doping as observed by Yeh *et al.* can be understood as a consequence of nesting driven magnetism. We are able to quantitatively explain the  $T = 0$  experimental data by use of band theoretical results, and have suggested a correlation between the Hall number and the residual resistivity. The quantitative success of the Fermi-surface nesting picture should provide a solid foundation for the eventual understanding of the finite temperature properties of V-doped Cr, which we do not treat in the current paper. More generally, V-doped Cr represents the first

known example of a nesting driven QCP, and further studies of this system can shed considerable new light on the more exotic QCPs, such as those seen in heavy fermion metals.

We would like to thank the authors of Refs. 8, 11, particularly Tom Rosenbaum and Anke Husmann, for communicating their work to us prior to publication, and permission to use their data in this paper. We also thank Dale Koelling for initial help with the band calculations, and Lucia Capogna for discussions concerning neutron data in  $Sr_3Ru_2O_7$  and Catherine Pepin concerning pseudogaps. This work was supported by the U. S. Dept. of Energy, Office of Science, under Contract No. W-31-109-ENG-38 (MRN, YB, RR) and by NSF Grant No. DMR-0090071, Robert A. Welch Foundation, and TC-SAM (QS). QS acknowledges the hospitality and support of Argonne National Laboratory, University of Chicago, University of Illinois at Urbana-Champaign, and KITP-UCSB.

- 
- [1] G. R. Stewart, *Rev. Mod. Phys.* **73**, 797 (2001).
  - [2] A. Schröder *et al.*, *Nature* **407**, 351 (2000).
  - [3] P. Coleman, C. Pepin, Q. Si, and R. Ramazashvili, *J. Phys. Cond. Matter* **13**, R723 (2001).
  - [4] Q. Si, S. Rabello, K. Ingersent, and J. L. Smith, *Nature* **413**, 804 (2001); *cond-mat/0202414* (2002).
  - [5] S. Paschen *et al.*, SCES2002 proceedings (2002).
  - [6] S. Chakravarty, C. Nayak, S. Tewari, and X. Yang, *Phys. Rev. Lett.* **89**, 277003 (2002).
  - [7] F. F. Balakirev, J. B. Betts, A. Migliori, S. Ono, Y. Ando, and G. B. Boebinger, preprint (2002).
  - [8] A. Yeh, Y.-A. Soh, J. Brooke, G. Aeppli, T. F. Rosenbaum, S. M. Hayden, *Nature* **419**, 459 (2002).
  - [9] J. M. Ziman, *Electrons and Phonons* (Oxford Univ. Pr., London, 1960), p. 502-503; T. P. Beaulac, F. J. Pinski, and P. B. Allen, *Phys. Rev. B* **23**, 3617 (1981); W. W. Schulz, P. B. Allen, and N. Trivedi, *ibid* **45**, 10886 (1992).
  - [10] J. Takeuchi, H. Sasakura, and Y. Masuda, *J. Phys. Soc. Japan* **49**, 508 (1980).
  - [11] M. Lee, A. Husmann, T.F. Rosenbaum, and G. Aeppli, to be published (2002).
  - [12] J. Schafer *et al.*, *Phys. Rev. Lett.* **83**, 2069 (1999).
  - [13] E. Fawcett, *Rev. Mod. Phys.* **60**, 209 (1988); E. Fawcett, H. L. Alberts, V. Yu. Galkin, D. R. Noakes, J. V. Yakhmi, *ibid* **66**, 25 (1994).
  - [14] The 2 by 2 secular matrix is exact for a helical SDW. This is not the case for the linear SDW, but one can show that in the case considered here, the linear result for  $\sigma_{xx}$ , etc., is approximately twice the helical result minus the paramagnetic result.
  - [15] T. M. Rice, *Phys. Rev. B* **2**, 3619 (1970).
  - [16] R.J. Elliott and F.A. Wedgwood, *Proc. Phys. Soc.* **81**, 846 (1963).
  - [17] R. Hlubina and T. M. Rice, *Phys. Rev. B* **51**, 9253 (1995).
  - [18] R. S. Perry *et al.*, *Phys. Rev. Lett.* **86**, 2661 (2001).
  - [19] L. Capogna *et al.*, *Phys. Rev. B* **67**, 012504 (2003).